Surface non-diamond carbon formation on laser patterned CVD diamond and its removal

John Smedley[a] and Triveni Rao
Brookhaven National Laboratory, Upton, New York 11973

Cherno Jaye and Daniel A. Fischer
National Institute of Standards and Technology, Gaithersburg, MD 20899

Jen Bohon
Case Western Reserve University, Cleveland, Ohio 44106

As diamond becomes more prevalent for electronic and research applications, methods of patterning diamond will be required. One such method, laser ablation, has been investigated in a related work.[1] We report on the formation of surface non-diamond carbon during laser ablation of both polycrystalline and single-crystal synthetic diamonds. Near edge x-ray absorption fine structure (NEXAFS) was used to confirm that the non-diamond carbon layer formed during the ablation was amorphous, and infrared absorption spectroscopy (FTIR) was used to estimate the thickness of this layer to be ~60nm. Ozone cleaning was used to remove the non-diamond carbon layer.

I. INTRODUCTION

Due to the unique combination of mechanical, optical, electronic and thermal properties, diamond is an ideal material for a wide variety of purposes. Recent advances in the chemical vapor deposition (CVD) process have increased the availability of high-purity diamond for optical, x-ray and electronic applications. For some of these applications, such as lenses[2] and diamond electron sources,[3] the diamond needs to be patterned with micron or sub-micron sized features. Although several techniques to etch diamond exist,[4-6] they are generally slow and prohibitive processes if significant thickness reduction or large aspect ratios are required. As an alternative and complimentary method, we have investigated laser ablation of both single- and poly-crystalline CVD diamond using laser pulses of ps and ns duration and wavelengths of 213, 266, 532 and 1064nm. The ablated samples were characterized using a number of techniques, including optical microscopy, SEM, AFM, FTIR, NEXAFS and x-ray diffraction. This manuscript is the second part of a series,[1] and details the chemical characterization.

This work describes the investigation of the non-diamond carbon (NDC) surface layer formed by laser ablation. The extent of NDC caused by laser ablation is characterized by two techniques, NEXAFS and FTIR. NEXAFS is sensitive to the bonding structure (sp2/sp3),[7] and thus determines the type of carbon in a given area. IR transmission through the ablated area, referenced to the transmission of bare diamond, allows an estimate of the thickness of the NDC layer. The prevalence of this layer was found to vary significantly with ablation parameters and diamond crystalline properties, however all diamonds tested exhibited some surface layer of NDC after ablation, both in the area of ablation and elsewhere on the diamond. Ozone cleaning was found to remove NDC efficiently, leaving a surface with a NEXAFS profile identical to the un-ablated diamond.

II. EXPERIMENTAL DETAILS

The NEXAFS measurements were performed at the NIST Soft X-ray beamline U7A of the National Synchrotron Light Source. The soft x-ray beam on the diamond samples was 0.5mm in diameter. The NEXAFS spectra were

measured by photoelectron emission using a retarding bias of 50V, yielding a sampling depth of 50nm.[8] All data were collected in partial electron yield mode with the signal normalized by the drain current of a clean gold I_0 mesh and energy calibrated using a second I_0 carbon mesh. For most samples, NEXAFS spectra were taken using a photon energy range of 260-330eV, around the carbon *K*-edge (284eV). For selected spots, survey scans were taken from 200eV to 1keV. All diamonds were sequentially ultrasonically cleaned in three 20-minute cycles, first in acetone, then ethanol, then DI water, and blown dry with nitrogen prior to data acquisition at the beamline. Data analysis was performed using the Athena program.[9]

The FTIR measurements were made at beamlines U2B & U2A at the NSLS, and the photoluminescence was done at U2A. The U2B FTIR measurements were performed using a Mercury-Cadmium-Telluride (MCT-A) detector (sensitive from 650-4000 cm^{-1}) through a Nic-plan IR microscope attached to a Magna 860 IR spectrometer (Nicolet/Thermo Fisher Scientific). Measurements were made in transmission mode with a resolution of $4cm^{-1}$ using the internal source apertured to produce a 100μm diameter spot on the sample. Data were processed using Omnic v7.3 (Nicolet/Thermo Fisher Scientific) and Excel (Microsoft, Inc.).

The carbon thickness calibration standards were created by the arc-deposition of carbon in the presence of 100mTorr argon gas onto a 2mm thick CaF_2 window using a CDS2.2 (Ladd Research) system at a current of ~60A. The window was placed ~4cm from the source to create a thickness gradient and was partially masked in order to form a carbon-non-carbon boundary for AFM measurements. The AFM measurements were made using an Easyscan 2 AFM (Nanosurf) to scan over a 66x66μm area with an image definition of 256 points per line at a speed of 1 second per line using a 225x40x7μm silicon ACLA-50 cantilever (AppNano) with a tip radius of <10nm and a tip height of 12-16μm at a frequency of 145-230kHz and a spring constant of 20-95N/m. The open-source software Gwyddion was used to process the data.

The diamonds were obtained from Element Six. Two grades of high purity diamonds were used: single-crystal (detector grade) and large grain polycrystalline (electronic grade). The detector grade diamond (S2) is $4x4mm^2$, with a thickness of 0.5mm. The electronic grade diamonds P1 and P2 are $10x10mm^2$ (P3 is $5x5mm^2$), with a thickness of 0.5 mm. Some diamonds required acid etching to remove NDC present on the surface upon receipt from the vendor. The acid etch consisted of a series of steps (personal communication, R. Stone), after each of which the diamond was rinsed in deionized water. These steps included: a 15 minute soak in saturated CrO_3 in H_2SO_4 (heated to produce vapors), 2 minutes of ultrasonic cleaning in 1:10 NH_4:H_2O, 2 minutes of ultrasonic cleaning in 1:10 HCl:H_2O, a 5 minute soak in boiling 5:1 H2SO4:H2O, 2 minutes in boiling 1:1:4 NH_4:H_2O_2:H_2O, and 2 minutes in boiling 1:1:4 HCl:H_2O_2:H_2O. Afterward, the diamonds were ultrasonically cleaned in deionized water and dried with nitrogen gas. Figure 1 shows the FTIR transmission spectra of detector grade and electronic grade diamonds as-delivered from the vendor, along with a type IIa natural diamond for comparison. The lack of measurable structure in the 1000-1300cm^{-1} region in the synthetic diamond spectra indicates that any nitrogen impurity[10] present is below the sensitivity limit of ~5ppm. Photoluminescence measurements on these diamonds also show that the impurity content is below the detection limit (data not shown). The specific details of the laser patterning procedure for each sample are addressed briefly in the results section and are described in detail in a related work.[1]

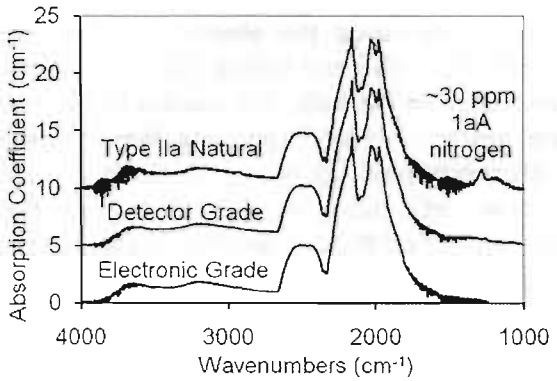

Figure 1. Infrared transmission spectra of natural type IIa diamond, detector grade (single-crystal) diamond and electronic grade (polycrystalline) diamond as received from the vendor. No nitrogen impurity is evident in the synthetic diamonds.

III. RESULTS AND DISCUSSIONS

A. NEXAFS Results

Reference standards

Bare diamond and amorphous carbon samples were measured for use as reference standards for the ablated diamonds. Figure 2 shows the pre- and post-edge normalized C *K* NEXFAS spectra for three detector grade diamonds. The first diamond was measured as delivered from the vendor, the second diamond was acid etched to remove NDC and the third diamond was ozone cleaned via exposure to a UV lamp (Jelight) at a distance of 1 cm for 4hrs per side. The spectra contain distinct spectral features, labeled (a-f). The 1s-π^* resonance at 285.5 eV is labeled (a), the sharp peak at 289.5 eV, labeled (b), is the diamond exciton on the rising edge of the 1s-σ^* resonance, labeled (c).[7,11,12] For pure diamond, the σ^* resonance should dominate, and the ratio of the intensity of (a) to (c) gives a figure of merit for the level of sp^2 to sp^3 bonding. The π^* resonance is still present in pure diamond due to surface reconstruction.[13] The second bandgap of diamond, labeled (d), appears at 302.4 eV. Another feature which is characteristic of diamond appears at 326 eV, and is labeled (e). For the as-delivered and ozone cleaned diamonds, two small features appear at 349.4 eV and 352.6 eV (labeled f), which indicate the presence of iron on the surface (second harmonic/order of the iron L3 and L2 absorption edges). For the ozone cleaned diamond, the ratio of a to c is 0.053, for the acid etched diamond, this ratio is 0.059 while for the as-delivered diamond it is 0.091, suggesting that the as-delivered diamond has some amount of NDC on the surface, which is removed by either acid etching or ozone cleaning.

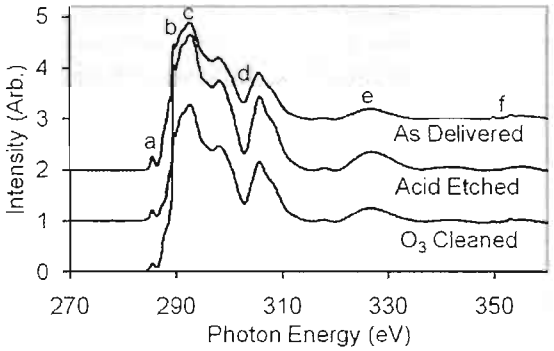

Figure 2. Normalized carbon *K* NEXAFS spectra for diamond as received from the vendor, an acid etched diamond and an ozone cleaned diamond. Labeled peaks correspond to a) the 1s-π^* resonance, b) the first diamond exciton, c) the 1s-σ^* resonance, d) the second diamond bandgap, e) an additional diamond feature and f) iron surface contaminants.

Figure 3 shows the normalized carbon *K* NEXAFS spectra of the amorphous carbon grid upstream of the sample and ablated regions of polycrystalline diamonds P1 and P3. The grid is used for wavelength calibration on the beamline; it also provides a reference spectrum for amorphous carbon with a large fraction of sp^2 bonds and lacking long range order. The diamond exciton and second band gap are absent, and the ratio of a to c is 0.67. Although there is some indication of the first exciton in the ablated region of P3, the signature diamond second band gap is entirely absent and the a to c ratio is 0.47. Based on these spectra, it is likely that the blackened surface of the ablated diamond is entirely NDC within the depth of NEXAFS observation (~50nm).[8]

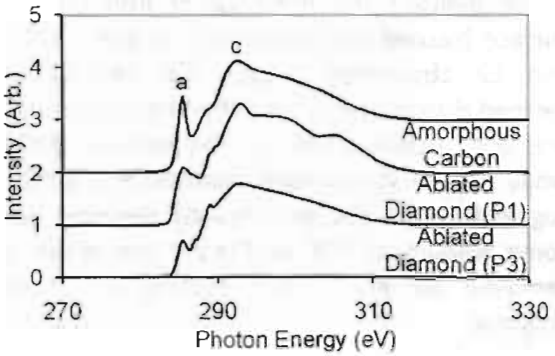

Figure 3. Non-diamond carbon NEXAFS spectra of an amorphous carbon grid (as standard reference) and regions of polycrystalline diamonds (P1 and P3) ablated with 266nm ps-duration radiation.

Ablation with ps pulse duration radiation

The details of laser ablation of diamond are described in detail in a related work;[1] for convenience, the names of the diamonds used in that work are retained here. For each ablated diamond, NEXAFS spectra were taken in the ablated region and in adjacent unablated areas. Figure 3 includes spectra for polycrystalline diamonds P1 and P3 ablated with 100μJ of 266 nm light, focused to a 27μm FWHM spot with a pulse duration of ~30ps FWHM. The ablation was performed using an iterated raster scan, producing a square ablated area 1 mm^2, large enough to accommodate the VUV beam for the NEXAFS measurement. Clear differences between the two diamond spectra in figure 3 are evident; this disparity indicates that the formation of NDC during ablation is not uniform, even when the same (bulk-sensitive) process is applied to two diamonds of the same grade. Ablated squares were created in vacuum as well as in various levels of oxygen, however the presence of oxygen during ablation (up to 100 Torr) did not affect the NEXAFS spectra; the ratio of a/c was 0.55±0.03 with no clear trend with changes in oxygen concentration.

Figure 4 shows the normalized carbon *K* NEXAFS spectra of polycrystalline diamond (P3) and single-crystal diamond (S2) ablated using 213nm light with similar beam properties (spot size, pulse duration) to those used for 266nm patterning. For this wavelength, the diamond is opaque, increasing the absorption of optical power at the diamond surface and reducing the absorption in the bulk. The spectra in figure 4 are nearly identical, suggesting that ablation with above band-gap energy produces a more uniform NDC layer on the surface of the diamond, regardless of whether the sample is single-crystal or polycrystalline.

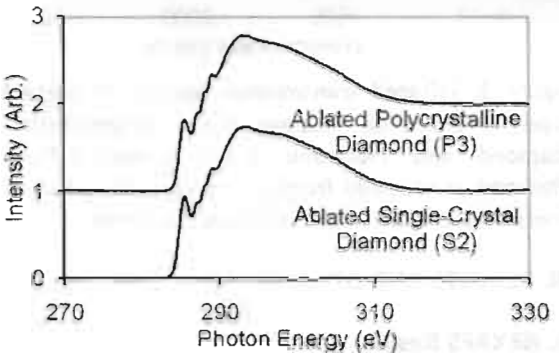

Figure 4. NEXAFS spectra of polycrystalline diamond (P3) and single-crystal diamond (S2) ablated with 213nm ps-duration radiation.

Ablation with ns pulse duration radiation

A polycrystalline diamond (P2) was ablated using similar energy density at 266nm, but with a pulse duration of 10ns FWHM. Various oxygen levels were used during ablation (up to 700 Torr), with no significant variation in the NEXAFS spectra (data not shown). In this case, the lines observed in the diamond were finer (although the same optical transport was used), leaving areas in the center of the pattern without the nearly opaque NDC coating characteristic of the other ablated diamonds. The diameter of the VUV beam used to measure the NEXAFS spectra was 0.5mm, much larger than the raster step of 50μm, thus the spectrum shown in figure 5 (black line) likely represents a combination of amorphous carbon and diamond. The grey line in figure 5 shows the theoretical fit of a linear combination of amorphous carbon and diamond standard spectra; the fit indicates that the spectrum is 15% diamond and 85% amorphous carbon.

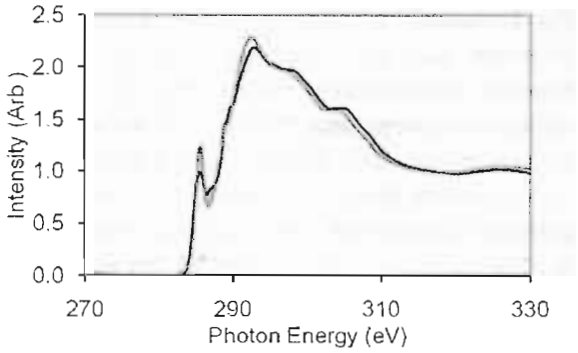

Figure 5. NEXAFS spectrum of polycrystalline diamond (P2) ablated with 266nm ns-duration radiation (black line). A linear combination fit of standard diamond and amorphous carbon to the data is shown in gray.

UV ozone cleaning

Two methods were investigated for the removal of NDC formed by laser ablation. The first was ablation in a molecular oxygen environment. As mentioned above, the presence of oxygen during the ablation did not impact the NDC formation. The second method investigated was post-ablation UV ozone cleaning. Ozone cleaning is a standard technique for removing radiation-induced graphitization of VUV optics.[14] A UV lamp (described above) was placed over diamond P1 for 6hrs, with a spacing of 1cm between the bulb and the diamond. After ozone exposure, the NDC was removed.

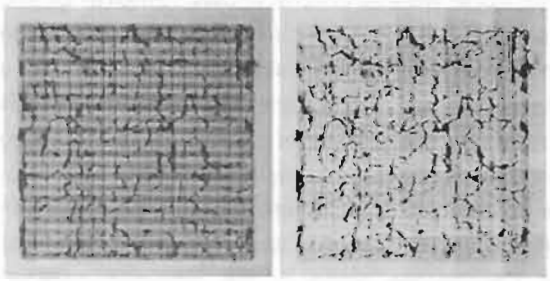

Figure 6. Optical microscope images of laser ablation pattern on P1 before (left) and after (right) UV ozone cleaning. The remaining dark areas in the cleaned diamond represent cracks extending into the bulk of the sample.

The visual appearance of the ablated area changed (Fig. 6) and the NEXAFS spectrum (Fig. 7) is consistent with bare diamond (Fig. 2). The form of carbon present was determined by comparison to literature,[7,11] and to measured standards of diamond and amorphous carbon.

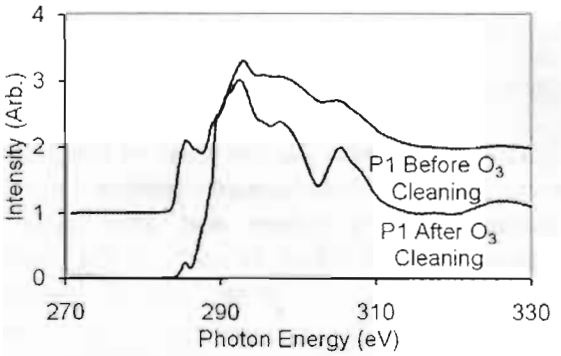

Figure 7. NEXAFS data for laser ablated area of P1 before and after UV ozone cleaning.

Initially, ablated areas of the diamond were compared to unablated areas to determine NDC formation, however the NEXAFS data for unablated diamond areas indicate that NDC deposits are not localized to the ablated areas, but extend to nearby regions (Fig. 8). Thus the data were fitted (Fig. 8, gray lines) using a linear combination of spectra from the amorphous carbon standard in figure 3 and from the ozone-cleaned control diamond sample in figure 2.

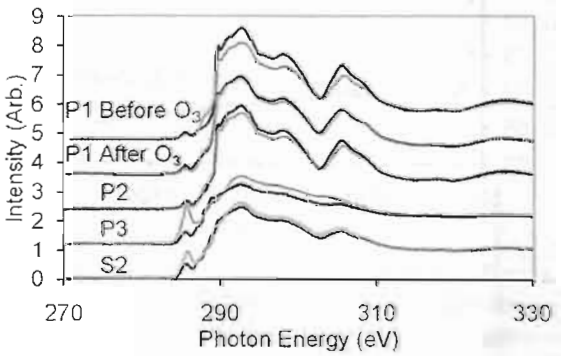

Figure 8. NEXAFS spectra of unablated regions of ablated diamonds as labeled (black lines). Linear combination fits of standard diamond and amorphous carbon to the data are shown in gray.

The larger diamonds (P1 and P2) provided ample area (100mm^2) within which to measure the unablated surface and fitting indicates 100% diamond spectra. Spectra measured on the smaller diamonds (P3 and S2) clearly show non-diamond carbon in the unablated area,

indicating only 12% diamond for P3 and 40% diamond for S2. The spectra were necessarily taken proximal to the ablated area due to the significantly smaller surface area ($16mm^2$) of these diamonds.

B. IR Results

In order to estimate the thickness of the NDC layer, infrared transmission spectra were measured for P1 before and after ozone cleaning. Spectra taken in each of the four ablated regions (avoiding cracks) were referenced to bare diamond areas of the same sample. Likely due to scattering effects from the roughened surface of the laser ablated area, the cleaned diamond did not transmit the IR radiation as well as the bare diamond. This effect resulted in an ~10% decrease in transmission for the cleaned laser patterned region referenced to bare diamond (Fig. 9), to which the P1 data before ozone cleaning has been normalized.

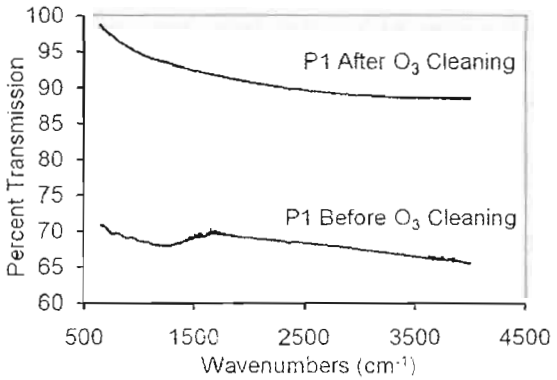

Figure 9. Infrared transmission spectra of the laser ablated region of P1 before and after UV ozone cleaning.

This spectrum represents an average of spectra from four patterned regions, however it should be noted that the individual spectra differ by an average of 20%, indicating significant inhomogeneity in the NDC deposition. Several forms of data verify that the NDC layer is completely removed (to below a measurable change in transmission), thus that the normalization is required. First, the NEXAFS data indicates the full removal of the NDC layer (Fig. 7). Second, a layer of carbon of a few nm in thickness was arc-deposited onto a calcium fluoride transmission slide; the deposited carbon was discernable by visual inspection, but did not measurably affect the IR transmission measurement (data not shown). P1 becomes optically transparent after ozone cleaning (Fig. 6). Third, the shapes of the IR transmission spectra with and without NDC differ significantly (Fig. 9); the cleaned diamond patterned region referenced to bare diamond is relatively featureless, while pre-cleaned P1 referenced to bare diamond exhibits structure attributable to the optical properties of the amorphous carbon.

It is particularly difficult to determine the thickness of an amorphous carbon layer, even with the aid of spectroscopic techniques.[15] In theory, the absorbance of the material at a given energy should be proportional to the thickness of the layer as determined by the absorption coefficient. Unfortunately, large baseline shifts in our calibration data ruled out the direct use of absorbance as a metric. However, during our investigations we noted that although the total absorbance of baseline shifted, the slope of the baseline was relatively stable. The same principles that apply to the direct comparison of absorbance to thickness also apply to the measurement of the slope, but the slope measurement allows removal of the unstable baseline level. In order to estimate the thickness of the NDC layer on the diamond, a slope calibration standard was required. For this measurement, a layer of carbon thick enough to provide reliable IR transmission data was arc-deposited onto a calcium fluoride transmission slide masked in such a way to create a gradient of thicknesses along a line between carbon-coated and clean CaF_2. AFM measurements were taken at two points along this line (Fig. 10) and IR transmission spectra were measured on the carbon coating proximate to these positions (Fig. 11).

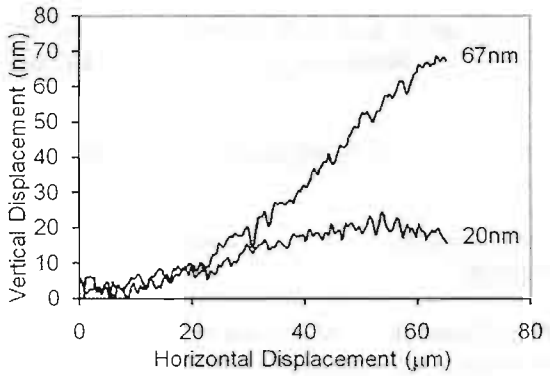

Figure 10. AFM scans of the boundary between clean CaF_2 and CaF_2 with carbon arc-deposited onto the surface. Thickness values measured were 67nm and 20nm.

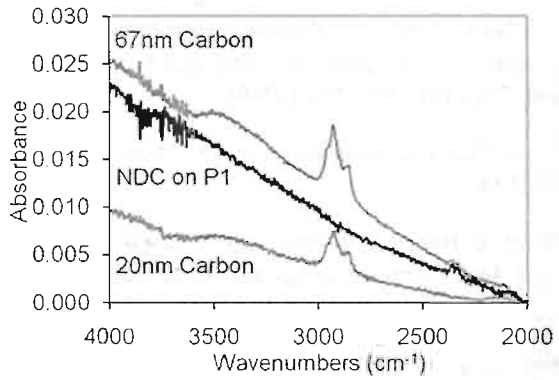

Figure 11. Infrared transmission spectra of arc-deposited carbon standards of 67 and 20nm thicknesses (gray lines) and averaged data from four spots on the laser ablated regions of P1 (black line) estimated to be ~60nm in thickness.

The peaks between 2800 and 3000cm^{-1} in the carbon standard spectra in figure 11 correspond to C-H stretching modes and occur in the standards because hydrogen is present during the carbon arc-deposition. The diamond ablation occurs in vacuum, so these peaks do not appear for the NDC formed on the diamond surface (Fig. 11, black). Due to the very small absorbances measured, significant error occurs due to minute fluctuation in baseline slopes. Using the slope of the worst baseline measured, this corresponds to a maximal 28nm error in the measurement. Based on these measurements, the layer of NDC is estimated to be 60±30nm thick in the laser patterned regions of P1 before ozone cleaning. The actual value is almost certainly near the higher end of this range, as the measurement depth of the NEXAFS technique is ~50nm and no significant diamond signature is evident in the spectra taken before ozone cleaning (Fig. 3).

IV. CONCLUSIONS

Based on the results of the study, we conclude that laser ablation of diamond to a depth of ~1μm results in non-diamond carbon formation on the ablated surface on the order of tens of nm in thickness under our experimental conditions. The effect is not entirely localized, as NDC deposits also occur away from the ablated area at a reduced thickness as well as on the windows of the vacuum system used for the ablation process. This is not surprising, as less than a tenth of the ablated material remains on the surface of the patterned region. NDC formation occurs for a variety of ablation laser parameters, both above and below the diamond band gap, and for both single and poly crystalline diamond. Below the diamond band gap, NDC may also be forming in the grain boundary regions of polycrystalline diamond. Above the band gap, the NDC layer is more uniform and is restricted to the surface. The form of NDC observed most closely resembles an amorphous carbon thin film created in vacuum. Ozone cleaning for a few hours effectively removes the NDC, leaving the bare diamond surface. These results indicate that laser ablation, preferably using above band gap radiation, may be used as a coarse file for diamond patterning and that the debris left behind is readily removed by UV ozone cleaning. Future investigations will include the use of reactive ion etching both as a tool for NDC removal and as a final step after ozone cleaning to attempt to smooth the ablated surface. A principal goal of diamond patterning is to create high aspect ratio features not currently achievable by reactive ion etching, thus future work will also include ablation of these types of features and verification that NDC can be as readily removed from these surfaces.

ACKNOWLEDGEMENTS

The authors would like to thank Qiong Wu for providing the AFM scans, John Warren for his assistance with carbon arc-deposition, John Walsh for his expert technical assistance and Veljko Radeka for his support. This manuscript has been authored by Brookhaven Science Associates, LLC under Contract No. DE-AC02-98CH10886 with the U.S. Department of Energy. The United States Government retains, and the publisher, by accepting the article for publication, acknowledges, a world-wide license to publish or reproduce the published form of this manuscript, or allow others to do so, for the United States Government purposes. Use of beamlines U2A, U2B and U7A at the National Synchrotron Light Source, Brookhaven National Laboratory, was supported by the U.S. Department of Energy, Office of Science, Office of Basic Energy Sciences, under Contract No. DE-AC02-98CH10886. Certain commercial names are mentioned in this manuscript for purpose of example and do not constitute an endorsement by the National Institute of Standards and Technology.

REFERENCES

[1]J. Smedley, T. Rao, Q. Wu and J. Bohon, J. Appl. Phys. **?**, ? (2009).

[2]K. Evans-Lutterodt, A. Stein, J. M. Ablett and N. Bozovic, Phys. Rev. Lett. **99**, 134801 (2007).

[3]J. Smedley, I. Ben-Zvi, J. Bohon, X. Chang, R. Grover, A. Isakovic, T. Rao and Q. Wu, *Diamond Amplified Photocathodes, in Diamond Electronics—Fundamentals to Applications II*, Mater. Res. Soc. Symp. Proc. 1039, Warrendale, PA, (2007), 1039-P09-02.

[4]J. Zhang, X. M. Meng, C. Y. Chan, Y. Wu, I. Bello, and S. T. Lee, Appl. Phys. Lett. **82**, 2622 (2003).

[5]H. W. Choi, E. Gu, C. Liu, C. Griffin, J. M. Girkin, I. M. Watson, and M. D. Dawson, J. Vac. Sci. Technol. B **23**, 130 (2005).

[6]M. Tarutani, Y. Takai and R. Shimizu, *Jpn. J. Appl. Phys., Part 2* **31**, L1305 (1992).

[7]F.L. Coffman, R. Cao, P. A. Pianetta, S. Kapoor, M. Kelly and L. J. Terminello, Appl. Phys. Lett. **69**, 568 (1996).

[8]Stöhr, J. NEXAFS Spectroscopy. Berlin: Springer-Verlag, 1992.

[9]B. Ravel and M. Newville, J. Synchrotron Rad. **12**, 537 (2005).

[10]W. R. Taylor, A. L. Jaques and M. Ridd, American Minerologist **75**, 1290 (1990).

[11]I. Gouzman, R. Shima-Edelstein, G. Comtet, L. Hellner, G. Dujardin, S. Roter and A. Hoffman, Diamond Rel. Mater. **8**, 132 (1999).

[12]D. M. Gruen, A. R. Krauss, C. D. Zuiker, R. Csencsits, L. J. Terminello, J. A. Carlisle, I. Jimenez, D. G. J. Sutherland, D. K. Shuh, W. Tong and F. J. Himpsel, Appl. Phys. Lett. **68**, 1640 (1996).

[13]M.-H. Tsai, J. C. Jiang and S. H. Lin, Phys. Rev. B **54**, 141 (1996).

[14]R. W. C. Hansen, M. Bissen, D. Wallace, J. Wolske and T. Miller, Applied Optics **32**, 4114 (1993).

[15]S. R. P. Silva, Properties of Amorphous Carbon. EMIS datareviews series, no. 29. London: INSPEC, 2003.